RFID Reader Receivers for Physical Layer Collision Recovery

Christoph Angerer, *Student Member, IEEE*, Robert Langwieser, *Member, IEEE*, and Markus Rupp, *Senior Member, IEEE*

***Abstract*—Arbitration and scheduling of multiple tags in state-of-the-art Radio Frequency Identification (RFID) systems is accomplished on the medium access control layer. Currently, only answers of a single tag can be decoded in such a system. If multiple tags respond simultaneously, a collision occurs. In that case, conventional systems discard the physical layer information and a retransmission is executed. This work shows how to recover from such collisions on the physical layer and successfully read the data. The contributions of the paper are: 1) An analysis of the achievable throughput increase of a system, that can recover from collisions at a physical layer is given. 2) A model for a description of collisions on the physical layer is presented. 3) Based on this model, we propose a channel estimation method and two types of receiver structures for separating the signals of a collision of two tags: first, single antenna receivers that discriminate the sources of the two tags in the I/Q plane, and second, multiple antenna receivers which exploit the different spatial signatures of both tags. 4) The functionality of the proposed receiver structures is verified with measurement data of two colliding tags. Eventually, a performance analysis of the receivers is provided.**

***Index Terms*—RFID, signal separation, collision recovery, MIMO, reader receivers, multi-user RFID.**

I. Introduction

RADIO Frequency Identification (RFID) is a wireless identification technology. We distinguish active and passive RFID systems, depending on the source of power supply of RFID tags. In passive systems, the tags absorb energy from an electromagnetic field provided by the RFID reader and use backscatter modulation for communication. Additionally, RFID systems are operated in various frequency domains: this work focuses on the Ultra High Frequency (UHF) domain at 860-950 MHz and follows the EPCglobal standard for passive UHF RFID [2].

All the RFID tags that are within the coverage area of the reader are scheduled using Framed Slotted Aloha (FSA) on the Medium Access Control (MAC) layer. Thereby, only slots with a single tag response can be decoded successfully, and in case of a collision at the air interface, the information is discarded [3].

However, recently different groups started to pay attention on slots with colliding RFID tag signals: Khasgiwale *et al*. [4] utilise information from tag collisions on the physical layer to estimate the number of tags involved in that specific collision slot. This information enhances the accuracy of RFID tag population estimators. Furthermore, the authors point out the potential to recover from collisions and correctly read the data of the colliding tags. Shen *et al*. [5] rigorously analyse signal constellations of colliding tag responses. In contrast to our work, they focus on Low Frequency (LF) tags. Their model is supported by measurement data, and they propose a recovery algorithm for tag collisions. Additionally, they simulate the error performance in case of multiple colliding tags. Yu *et al*. [6] combine beamforming with anti-collision techniques, separating the tag population into sectors and running FSA or binary tree search in each sector, but do not try to recover from collisions. Lee *et al*. [7] identify the potential performance increase by combining smart antennas with binary tree and Slotted Aloha anti-collision algorithms, while this work focuses on FSA as defined in [2]. Finally Mindikoglu *et al*. [8] develop a blind multiple antenna signal separation receiver for RFID collision recovery, based on the zero constant modulus algorithm. In contrast to their work, our receivers require a channel estimate, which is proposed in this paper. In their paper, they focus on compensation of a residual carrier offset, which in general is not present in RFID, as pointed out in Section III.

In this work, we exploit the specific characteristics of RFID systems to separate signals from collisions at the physical layer. We discuss the theoretical performance increase of an FSA system with the capability of recovering from collisions at the physical layer in the following Section II. In Section III we accurately model tag collisions and constellations in the baseband of the receiver. With such a model, we propose a channel estimation method and propose two classes of receivers that are capable of recovering from collisions in Section IV. To the best knowledge of the authors, these receivers are the first to be proposed for separating UHF RFID tag signals of collision slots. Both of these receiver classes are tested on measurement data of collisions in Section V. A performance analysis of the proposed receivers is provided in Section VI. The last section finally concludes the paper.

Paper approved by D. I. Kim, the Editor for Spread Spectrum Transmission and Access of the IEEE Communications Society. Manuscript received January 4, 2010; revised May 3, 2010.

Some parts of the work were published in [1]: C. Angerer, G. Maier, M. V. Bueno-Delgado, M. Rupp, and J. Vales- Alonso, "Single antenna physical layer collision recovery receivers for RFID readers," was published in the Proceedings of the IEEE International Conference on Industrial Technology, Viña del Mar, Chile, March 2010.

The authors are with the Institute for Communications and Radio Frequency Engineering, Vienna University of Technology, Gusshausstrasse 25/389, 1040 Wien, Austria (e-mail: {cangerer, rlang, mrupp}@nt.tuwien.ac.at).

Digital Object Identifier 10.1109/TCOMM.2010.101910.100004

TABLE I
TERMS AND PARAMETERS

Variable	Description
N	number of tags within the read range
K	frame-size or total number of slots
R	number of tags transmitting in the same slot
M	number of tags the reader is capable to resolve
J	number of tags the reader is capable to acknowledge
$i \in [1 \dots R]$	tag index
N_R	number of receive antennas at the RFID reader
$j \in [1 \dots N_R]$	antenna index
$E\{\mathcal{X}\}$	expected value of the random variable $\mathcal{X}$
h^*	conjugate complex of h
$\mathbf{H}$	bold terms indicate vectors or matrices
$\mathbf{H}^H$	Hermitian transpose of the matrix $\mathbf{H}$

II. Framed Slotted Aloha with Physical Layer Collision Recovery

Several RFID standards, as the EPCglobal standard for UHF RFID [2], apply Framed Slotted Aloha to arbitrate the air interface and to schedule the transmission of a tag population of N tags. For convenience, Table I provides a description of the most important parameters and terms used in this paper. In FSA systems, the reader starts a frame with K slots, issuing a `QUERY` command, which announces the frame size K. The tags randomly select one of these following slots for transmission, whose start is indicated by `QUERY_REP` commands from the reader. The response of the tags to these `QUERY` and `QUERY_REP` commands is a 16 bit random number. Note that this random number in the response is *not* related with the randomly picked slot. This random number is acknowledged by the reader as a handshake mechanism. Upon reception of a correct acknowledge, the arbitration process is finished and the tag returns its unique identifier. After the communication with the tag is finished, the reader announces the start of the following slot [2].

It may occur that certain slots are not used by tags for transmitting their random number (empty slots), some are used by one tag (singleton slots) or even more than one tag (collision slots), causing a collision at the air interface. Let $\mathcal{X}_R$ be a random variable indicating the number of slots with exactly R tag responses. Then, the expected number of slots with exactly R tags transmitting is given by:

$$E\{\mathcal{X}_R\} = K\binom{N}{R}\left(\frac{1}{K}\right)^R\left(1-\frac{1}{K}\right)^{N-R}, \qquad (1)$$

where $E\{\cdot\}$ denotes the expected value. Conventional RFID readers only can read data in singleton slots, leading to the well known maximum average throughput of $\frac{E\{\mathcal{X}_1\}}{K} = 0.368$ successful readouts per slot [9]. This throughput is achieved if the frame size is set equal to the tag population size ($K = N$), as indicated in Fig. 1.

However, if it is possible to recover from a slot with $R \leq M$ colliding tags, we only encounter an unreadable slot if more than M tags transmit in the same slot. We first consider the case that the reader picks out one of these R tags and acknowledges this single tag, while the other received tag responses are discarded. Then, in each slot with $R \leq M$ one tag is identified, and hence the average throughput $T = \frac{1}{K}\sum_{R=1}^{M} E\{\mathcal{X}_R\}$ can

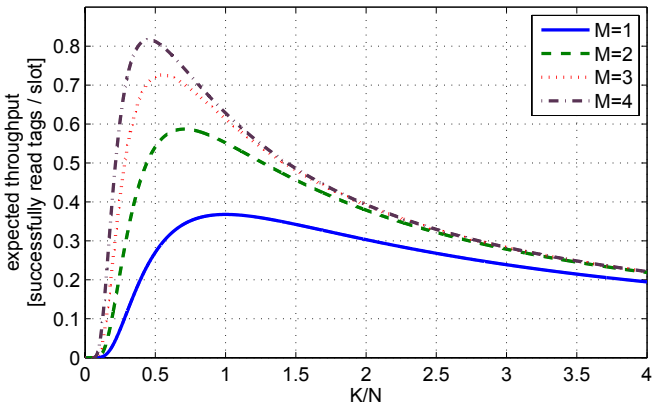

Fig. 1. Expected throughput for $J = 1$, depending on frame size to tag ratio K/N.

TABLE II
OPTIMAL FRAMESIZE K_{opt} AND EXPECTED THROUGHPUT FOR READERS RESOLVING $M = 1 \dots 4$ COLLISIONS ($J = 1$)

M	K_{opt}/N	expected throughput	relative improvement
1	1	0.368	1.000
2	0.707	0.587	1.595
3	0.550	0.726	1.973
4	0.452	0.817	2.220

be directly computed from Equation (1) by:

$$T = \sum_{R=1}^{M}\binom{N}{R}\left(\frac{1}{K}\right)^R\left(1-\frac{1}{K}\right)^{N-R}. \qquad (2)$$

In order to maximise the average throughput the optimal frame size K_{opt}, can readily be derived by solving the following equation:

$$\sum_{R=1}^{M}\binom{N}{R}\left(\frac{1}{K_{opt}}\right)^{R+1}\left(1-\frac{1}{K_{opt}}\right)^{N-R-1} \times\left(\frac{N}{K_{opt}}-R\right) = 0. \qquad (3)$$

Figure 1 shows the expected throughput of receivers being capable to recover from collisions with up to M tags, for $N = 10^4$. Compared to a conventional reader ($M = 1$), a reader that is able to recover from a collision with up to $M > 1$ tags adjusts a shorter frame size for maximal throughput. This result is intuitive, as a reader with e.g. $M = 2$ maximises the expected number of slots with a single ($R = 1$) and two responses ($R = 2$), while a conventional reader just maximises the expected number of singleton slots.

Clearly, the expected throughput increases with the parameter M, and converges toward one successfully read tag per slot for $M \to \infty$. The optimal values of frame sizes related to the tag population size and the average throughput is shown in Table II for $M = 1, \dots, 4$. A reader with the capability to recover from a collision with two tags ($M = 2$), already achieves a theoretical increase of the expected throughput of 1.6 times the throughput of a conventional reader, motivating the development of such a receiver. We develop a signal model for collisions in the following Section III, and propose corresponding reader receiver architectures with $M = 2$ in Section IV.

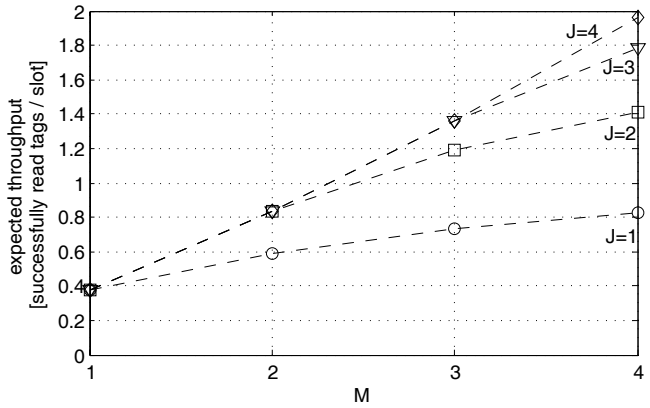

Fig. 2. Expected throughput with optimal frame size settings for a reader with the capability to recover from a collision with M tags and to acknowledge up to J tags.

Until now we have considered the case where the reader selects one out of the decoded tags in a collision slot with $R \leq M$ tags and acknowledges only this tag, while the other received signals are discarded. If however the reader additionally manages to acknowledge up to J tags simultaneously (J out of the M received tags, $J \leq M$), the theoretical throughput is further increased to:

$$T = \sum_{R=1}^{J} \binom{N}{R} \left(\frac{1}{K}\right)^{R} \left(1-\frac{1}{K}\right)^{N-R} R + \sum_{R=J+1}^{M} \binom{N}{R} \left(\frac{1}{K}\right)^{R} \left(1-\frac{1}{K}\right)^{N-R} J. \quad (4)$$

Similarly to the derivation above, we can calculate the optimal framesize and expected throughput. Figure 2 shows the expected throughput depending on the two parameters M and J. Acknowledging multiple received tags may be accomplished by exploiting the spatial separation of the tags on the transmitter by means of precoding with multiple transmit antennas [10, Chapter 8]. This requires at least partial knowledge about the forward channel, which may be extracted from the backward channel estimate, especially if the forward and backward channel exhibit a strong correlation [11], [12]. Such a strong correlation is expected if the same antennas are transmitting and receiving. Moreover, the acknowledgment of multiple received tags may also be achieved by changing the standard to allow the acknowledgment of multiple tags consecutively. In this paper we however only focus on receivers for recovering from tag collisions and leave precoding at the transmitter for future work.

III. Signal Constellations in Tag Collisions

A. Signal Model of Collisions on the Channel

Figure 3 shows the basic communication between several tags and an RFID reader, equipped with N_R receive antennas. In passive RFID systems the communication is half-duplex, and during times the reader does not modulate any signal, it provides the RFID tags with energy in form of a continuous carrier transmission. While passive tags absorb energy from that field, the carrier transmission also leaks into the N_R receive paths of the RFID reader. This carrier leakage at receive antenna j results in:

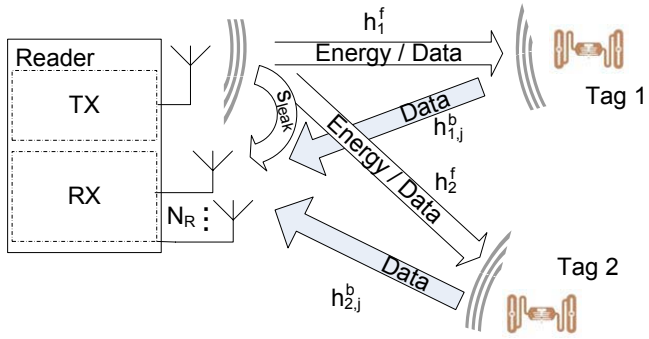

Fig. 3. Communication between a reader and two tags.

$$s_j^{leak}(t) = |L_j| \sin(\omega_c t + \varphi_j^{leak}). \quad (5)$$

Here $\omega_c = 2\pi f_c$, and f_c denotes the carrier frequency of the transmitted wave of the reader. The phase shift φ_j^{leak} results from the propagation delay between the transmit and the j'th receive antenna, while the amplitude $|L_j|$ of the leakage is determined by the decoupling between the transmit and j'th receive antenna, which is assumed to be constant during one transmission.

For transmitting information to the reader, tags use backscatter modulation. Given R tags transmitting in a certain slot, each tag i ($i \in [1 \dots R]$) changes from absorbing energy (tag absorb state, $S^{(a)}$) to reflecting energy (tag reflect state, $S^{(r)}$), by mismatching their antenna input impedance. This backscattered signal is given by:

$$s_{tag,i}(t) = |h_i^f| \sqrt{|\Delta\sigma_i|} a_i(t) \sin(\omega_c t + \varphi_i^f + \varphi_i^{\Delta\sigma}), \quad (6)$$

where $|h_i^f|$ and φ_i^f are the forward (reader to tag) channel attenuation and phase shift, respectively. The term $\varphi_i^{\Delta\sigma}$ describes the phase shift introduced by the modulation of tag i, while $|\Delta\sigma_i|$ is the normalised differential radar cross section as described by Nikitin *et al.* [13], which basically describes the modulation efficiency:

$$|\Delta\sigma_i| = |\rho_i^r - \rho_i^a|^2, \quad (7)$$

where ρ_i^r and ρ_i^a are the complex reflection coefficients for the reflect and absorb state of tag i, respectively. According to the EPCglobal standard [2], each tag modulation signal $a_i(t)$ realises an on-off keying ($a[k] \in [0, 1]$), and features a different modulation frequency (by a different symbol period T_i) and a distinct delay τ_i delaying the start of the modulation phase:

$$a_i(t) = \sum_k a_i[k] p(t - kT_i - \tau_i). \quad (8)$$

Here, $a_i[k]$ and $p(t)$ denote the transmitted symbol and the pulse shape of the modulation signal, respectively. For the sake of a simple model, we neglect the noise in the forward link and model all noise of the system as additive white Gaussian pass-band noise $n_j^{pb}(t)$ at antenna j in the backward channel. Thus, at the $j'th$ antenna the R backscattered signals of the

collision slot are distorted by the carrier leakage and noise:

$$s_j^{pb}(t) = \sum_{i=1}^{R} |h_{i,j}^b| \sqrt{|\Delta\sigma_i|} a_i(t) |h_i^f| \sin(\omega_c t + \varphi_i^f + \varphi_i^{\Delta\sigma} + \varphi_{i,j}^b) + s_j^{leak}(t) + n_j^{pb}(t). \quad (9)$$

The backward (tag-to-reader) channel between each tag i and receive antenna j inserts the attenuation $|h_{i,j}^b|$ and phase shift $\varphi_{i,j}^b$. In our model we assume that the channel attenuations $|h_i^f|$, $|h_{i,j}^b|$ and phase shifts φ_i^f $\varphi_{i,j}^b$, as well as the tag modulation parameters $\sqrt{|\Delta\sigma_i|}$ and $\varphi_i^{\Delta\sigma}$ do not change significantly during the transmission of one packet (block fading, readout duration $\approx 50\mu s$).

B. Constellations in the Baseband of the Receiver

After receiving the collided signals at the antennas, the reader first downconverts the receive signals to the baseband. Hence, the complex-valued baseband signal at receive antenna j is:

$$s_j(t) = \sum_{i=1}^{R} h_{i,j}^b \sqrt{\Delta\sigma_i} a_i(t) h_i^f + L_j + n_j(t), \quad (10)$$

with $h_i^f = |h_i^f| e^{j\varphi_i^f}$ and $h_{i,j}^b = |h_{i,j}^b| e^{j\varphi_{i,j}^b}$ denoting the complex-valued channel coefficients, $\Delta\sigma_i = |\Delta\sigma_i| e^{j2\varphi_i^{\Delta\sigma}}$ is the complex-valued normalised differential radar cross-section, $L_j = |L_j| e^{j\varphi_j^{leak}}$ denoting the complex-valued carrier leakage and $n_j(t) = n_j^{pb}(t) e^{j\omega_c t}$ denoting the complex-valued noise at each antenna j with noise power spectral density N_0. Stacking the receive signals of each antenna into a vector, we can rewrite:

$$\mathbf{s}(t) = \mathbf{H}^b \mathbf{S} \mathbf{A}(t) \mathbf{h}^f + \mathbf{l} + \mathbf{n}(t). \quad (11)$$

Here $\mathbf{s}(t)$, $\mathbf{l}$ and $\mathbf{n}(t)$ are the $N_R \times 1$ column vectors with the elements $s_j(t)$, L_j and $n_j(t)$, respectively. The term $\mathbf{H}^b$ denotes the $N_R \times R$ tag-to-reader channel matrix with elements $h_{i,j}^b$ in row j and column i, $\mathbf{A}(t)$ and $\mathbf{S}$ are the $R \times R$ modulation and radar cross-section matrices with $a_i(t)$ and $\sqrt{\Delta\sigma_i}$ as their diagonal elements and 0 elsewhere, respectively, and $\mathbf{h}^f$ is the $R \times 1$ vector with the forward channel coefficients h_i^f. Equation (11) can be equivalently reformulated to:

$$\mathbf{s}(t) = \mathbf{H} \mathbf{a}(t) + \mathbf{l} + \mathbf{n}(t), \quad (12)$$

where $\mathbf{H} = \mathbf{H}^b \mathbf{S} \mathrm{diag}(\mathbf{h}^f)$ represents the equivalent $N_R \times R$ channel matrix with the elements $h_{i,j} = h_i^f h_{i,j}^b$, $\mathrm{diag}(\mathbf{h}^f)$ is the $R \times R$ diagonal matrix with the elements h_i^f on its diagonal, and $\mathbf{a}(t)$ is the $R \times 1$ modulation vector with the elements $a_i(t)$.

The system describes basically a multi-user system, with the following important properties:

- First, all signal components are modulated by the same carrier frequency, which originates from a *single* source, namely the transmitter of the reader. This important property inherent in backscatter technology makes it *feasible to jointly-downconvert* all signal components with the same modulation frequency.

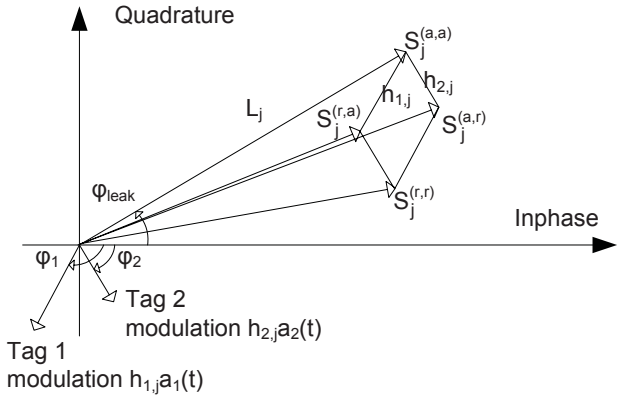

Fig. 4. Reader baseband I/Q diagram of collision of two tags at antenna j.

- Second, the modulation signals feature a different symbol rate, which deviates up to $\pm 22\%$ between the single tags in a UHF RFID system [2]. This strong deviation is not present in High- and Low Frequency (HF / LF) RFID systems, as the symbol clock is derived from the carrier frequency in these systems. In contrast to that, UHF RFID tags exhibit an oscillator, which on the one hand drifts with the supply voltage, and on the other hand exhibits a relatively low frequency (e.g. 1.92 MHz), leading to a coarse time resolution for generating the data rate in the defined continuous frequency range from 40 kHz to 640 kHz [14], [15]. Additionally, each tag starts its modulation phase at a different time, as indicated by the delay τ_i terms in Equation (8). This asynchronism makes it *unfeasible to jointly sample* all the signals with a single symbol rate.
- Finally the tag receive signals are impaired by the carrier leakage and noise. In a practical system, this carrier leakage can be up to 90 dB stronger than the backscattered signal [16].

Figure 4 shows the constellation of two colliding tags in the baseband I/Q plane of one antenna j of the reader receiver: While both tags absorb energy, the reader only discovers the carrier leakage absorb state of both tags, $S_j^{(a,a)} = L_j$. If Tag 1 backscatters information to the reader, this signal adds with the carrier interference and gives a second state in the I/Q plane, the Tag 1 reflect state and Tag 2 absorb state $S_j^{(r,a)} = L_j + h_{1,j}$. The vice-versa situation, where Tag 1 absorbs energy while Tag 2 reflects energy, realises the point $S_j^{(a,r)} (= L_j + h_{2,j})$, and finally, if both tags reflect energy simultaneously, the state $S_j^{(r,r)} = L_j + h_{1,j} + h_{2,j}$ is generated. In general, we find up to 2^R different states. Hence, the number of different states generated in the I/Q plane indicates the number of tags participating in the collision [4], [5], which can be utilised to enhance tag population estimators [17].

The location of the constellation in the I/Q plane depends on the phase and amplitude of the carrier leakage and on the channel coefficients. In general, the various states of the constellation in the I/Q plane of the receiver are unknown and arbitrary to the reader receiver.

We assume that tags switch between their absorb and reflect state according to a rectangular modulation function with the

basic frequency defined as the backscatter link frequency [2]. For realising the two states, tags basically switch their shunt transistor on and off, and due to their simplicity other pulse shapes than rectangular are technologically not feasible. In order to maximise the receive E_b/N_0, we apply a matched filter which is realised by an integration over a half backscatter link frequency period. This changes the pulse shape of the tag modulation signal from rectangular to triangular. Hence, the signal moves between the states indicated in Fig. 4. Additionally, due to the asynchronous modulation signals of the tags, the receive signals move basically within the entire area between the four states. On the other hand, two synchronous tags only move on straight trajectories between the various states (as this is the case in the example of Fig. 5).

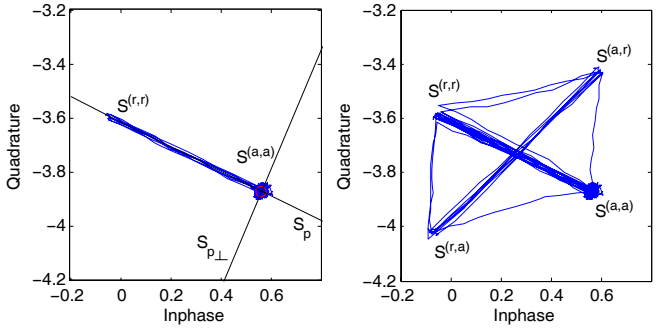

Fig. 5. Channel estimation: simulated constellation during preamble and entire RN16 transmission for two synchronous tags.

IV. Collision Resolving Receivers

With the above developed model in mind, we are now ready to develop two different classes of receiver structures:

- As a first class of receivers we propose Single Antenna (SA) receivers. These receivers discriminate the signal components from the two tags participating in the collision in the I/Q plane and are capable to recover from a collision with at most two tags.
- As a second class of receivers we propose multiple receive antenna receivers. These receivers exploit the spatial domain in order to discriminate between the signal components of the two tags. We focus here on dual receive antenna receivers, also capable of recovering from slots with two tags at most.

Both classes of receivers separate the signals in the collision slot into the components corresponding to the single tags. Synchronisation and decoding is thereafter performed for each resolved tag signal individually. This circumvents joint sampling, as all resolved tag signals may be sampled with their respective symbol frequency. As both classes of receivers require channel knowledge, a technique for estimating the channel at each antenna j for a collision slot with two tags is proposed first.

A. Channel Estimation

Reviewing Equation (12), we find the two tag signals of interest, degraded with the carrier leakage and noise at each antenna. While the tag signals are only active during times of backscatter modulation, the carrier is always leaking into the receiver. Assuming a static carrier leakage during one tag transmission, we can first estimate this leakage during times where both tags are in their absorb state $S_j^{(a,a)}$. Such a period is defined in [2] (and similarly by others) immediately before the tags respond (defined as T_1). In a digital receiver we can utilise this period to estimate the carrier interference ($L_j = S_j^{(a,a)}$) as the temporal mean during that interval T_1 [18]:

$$\hat{S}_j^{(a,a)} = E\{s_j[k]\}_{T_1}, \tag{13}$$

$E\{\cdot\}_{T_1}$ denotes the averaged value over time period T_1, and k is the sample index.

Tag sequences start with a defined preamble. Hence, all tags modulate the same bits at the beginning. Although the tags may start with a distinct delay τ_i (compare with Equation (8)), the delay between two tags $\tau_1 - \tau_2$ is smaller than a half pulse period [2]. As the first symbol of the preamble has a steady level in the standardised FM0 encoding, we can estimate the state $S_j^{(r,r)}$ during this first symbol of the preamble (t_{1bit}), which is determined at the largest deviation from $S_j^{(a,a)}$ in the I/Q plane:

$$\hat{S}_j^{(r,r)} = \max\left\{|s_j[k] - \hat{S}_j^{(a,a)}|\right\}_{t_{1bit}}. \tag{14}$$

As stated above, a matched filter is applied to the receive signal, which integrates the signal over one half symbol period and thus changes its shape from rectangular to triangular. The peaks of this triangular function thus serve as an estimate of the average over half a symbol interval of the reflection state. During the preamble, the receive signal moves between the two states $S_j^{(a,a)}$ and $S_j^{(r,r)}$, as shown in the left plot of the simulated constellation in Fig. 5.

Finally, the realisation of the remaining states $S_j^{(a,r)}$ and $S_j^{(r,a)}$ depends on the generated data (16 bit random numbers, RN16). As soon as both tags modulate different data, these two states are realised. If only one tag responds in a certain slot, the receive signal is composed of two states and lies in a one-dimensional subspace of the I/Q plane defined by the absorb and reflect state of that tag. This subspace S_P is realised, and the two states are estimated, during the transmission of the preamble. However, if several tags generate a collision, we also find signal components in the orthogonal subspace $S_{P\perp}$ of the preamble subspace S_P. These two orthogonal subspaces are indicated by the lines in the left plot of Fig. 5. The states $S_j^{(a,r)}$ and $S_j^{(r,a)}$ are then estimated at the points with maximal signal strength in this orthogonal subspace component:

$$\hat{S}_j^{(a,r)} = \max_k\{s_\perp[k]\}, \quad \hat{S}_j^{(r,a)} = \min_k\{s_\perp[k]\}. \tag{15}$$

Here, $s_\perp[k]$ denotes the signal component located in $S_{P\perp}$. It is insignificant if we exchange $S_j^{(a,r)}$ and $S_j^{(r,a)}$ in our estimation, as it is irrelevant which decoded signal belongs to which tag.

As the modulation signals $a_1(t)$ and $a_2(t)$ are assumed to realise perfect on-off keying, the channel coefficients directly correspond to:

$$\hat{h}_{1,j} = \hat{h}_1^f\sqrt{\Delta\sigma_1}\hat{h}_{1,j}^b = \hat{S}_j^{(r,a)} - \hat{S}_j^{(a,a)}, \tag{16}$$

$$\hat{h}_{2,j} = \hat{h}_2^f\sqrt{\Delta\sigma_2}\hat{h}_{2,j}^b = \hat{S}_j^{(a,r)} - \hat{S}_j^{(a,a)}. \tag{17}$$

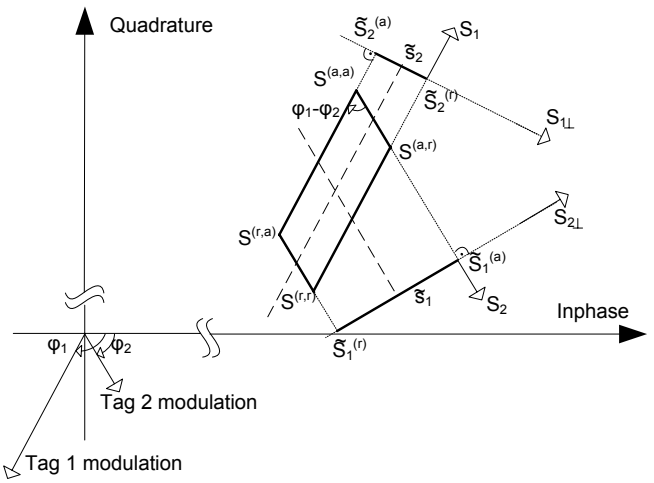

Fig. 6. Single Antenna Zero-Forcing (SAZF) receiver with projection of the constellation into the orthogonal subspace of the interference.

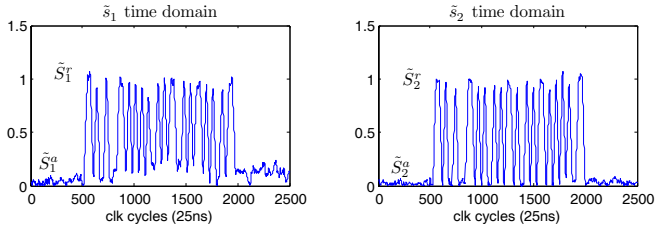

Fig. 7. Recovered tag signals with single antenna ZF receiver (measurement data).

In summary, the receiver distinguishes between one ($R = 1$) or more than one ($R > 1$) receive signals whether there is a signal component in the subspace $S_{P\perp}$. The proposed channel estimation allows for an estimation of the states for two colliding tags, thus M is restricted to two with this algorithm. Clearly, if more tags generate a collision, a separation of the signals into two orthogonal subspaces is not sufficient to estimate all the generated states. In the case of more than two colliding tags ($R > 2$), the reader may estimate the states incorrectly, leading a fault readout of the tag data (RN16), which in general always happens for $R > M$. In that case, the acknowledged data is wrong, terminating the communication with the tags. As expected, this case (collision slot $R > M$) leads to a throughput of zero tags in that certain slot. The access of the unread tag is handled by the protocol: All tags that are not acknowledged, again participate in the following arbitration frame [2].

This work treats the channel estimation for collisions of two tags, an estimation for collisions of more tags is left for future work. This may be approached without applying a matched filter, but directly sampling the rectangular-shaped baseband signal [4], [5]. Then, the baseband samples only realise the states corresponding to the various combinations of reflection and absorption at all the tags (as the transitions are instantaneous). However, matched filtering allows to diminish the noise bandwidth considerably, as the supported bandwidth is much smaller than in case of representing the rectangular signal shape. Therefore, this approach sacrifices on E_b/N_0, and non-synchronous tags still hamper this approach, as states do not change with a single symbol rate.

B. Single Antenna Receivers

1) Single Antenna Zero-Forcing (SAZF) Receiver: The first proposed receiver capable of recovering from a slot with two tags colliding, is a single antenna zero-forcing receiver. It separates one signal from the constellation by treating the other as interference. The signal constellation is projected into the (one-dimensional) subspace that completely cancels the interference, i.e. the subspace ($S_{i\perp}$) orthogonal to the interfering component (S_i, see Fig. 6). These projected signals $\tilde{s}_i$ move between the projected states $\widetilde{S}_i^a$ and $\widetilde{S}_i^r$. The projection $\tilde{s}_i$ of each tag signal is thereafter synchronised, sliced and decoded separately (Fig. 7).

This projection also degrades the signal strength of the desired signal, while the noise power in the projected component remains equal. Hence also the Signal to Noise Ratio (SNR) is degraded by the projection. The degradation of the signal strength depends on the angle between the two tag modulation signals and is proportional to $\sin(\varphi_1 - \varphi_2)$, where $\varphi_i = \varphi_i^f + \varphi_i^{\Delta\sigma} + \varphi_i^b$. Hence, if the two tag signals transmitting in the slot are close to orthogonal in the I/Q plane, the loss is small. However if the angles of the receive signals are almost equal, a high fraction of receive signal power is lost by this projection. Reviewing our signal model, we find that the angle $\varphi_1 - \varphi_2$ is random to the receiver and distributed uniformly in $(-\pi, \pi]$.

The zero-forcing receiver can also be interpreted as a receiver, setting two separate decision thresholds inside the area spanned by the four constellation points $S^{(a,a)}$, $S^{(a,r)}$, $S^{(r,a)}$ and $S^{(r,r)}$, as indicated by the dashed lines in Fig. 6. These decision regions are different from those of a maximum likelihood receiver. As mentioned above, the four expected constellation points are only realised if both tags realise a certain state simultaneously. Due to the asynchronous symbol rates of both tags however, the signal moves inside the area spanned by the four states, making a decision in the decision regions of the maximum likelihood receiver infeasible.

We underline, that this receiver is only capable of recovering from slots with two tags. If more than two tags create the signal constellation, it is not possible to find a subspace $S_{i\perp}$ which is orthogonal to both interferers in the two-dimensional I/Q space.

2) Single Antenna Ordered Successive Cancellation (SAOSUC) Receiver: Furthermore, we propose a single antenna ordered successive cancellation receiver, that is decoding the streams sequentially. First it selects the stream with higher receive signal power (reflected by h_i), which is first decoded by the zero-forcing receiver as described above. Thereafter, the result is remodulated and subtracted from the signal constellation. Assuming the decision process was correct, the interference for the second stream is canceled [19]. Hence, the remaining signal is only composed of the signal component of the second tag. In a final step the remaining signal is sliced separately. This receiver exploits the fact, that the above described projection loss just affects the signal that is decoded first.

C. Multiple Antenna Receivers

1) Zero-Forcing (ZF) Receiver: In order to separate the signal components exploiting multiple receive antennas, we first propose the well known zero-forcing receiver [10]:

$$\hat{\mathbf{s}}_{ZF} = (\hat{\mathbf{H}}^H \hat{\mathbf{H}})^{-1} \hat{\mathbf{H}}^H (\mathbf{s} - \hat{\mathbf{l}}). \tag{18}$$

The superscript $\mathbf{H}^H$ denotes the Hermitian transpose (conjugate transpose) of the matrix $\mathbf{H}$. In contrast to the single antenna receiver, it exploits the different spatial signatures in order to separate the signals. Thus, the receiver does not suffer from a projection loss.

2) Minimum-Mean-Square-Error (MMSE) Receiver: It is well known in literature [10], that the zero-forcing receiver suffers from a noise enhancement due to the inversion of the matrix $\mathbf{H}^H\mathbf{H}$. The MMSE receiver takes into account both, the interference and the noise, and balances the error:

$$\hat{\mathbf{s}}_{MMSE} = \mathbf{G}(\mathbf{s} - \hat{\mathbf{l}}) + \mathbf{c}, \tag{19}$$

with

$$\begin{aligned} \mathbf{G} &= \hat{\mathbf{H}}^H (\hat{\mathbf{H}}\hat{\mathbf{H}}^H + 4N_0\mathbf{I})^{-1}, \\ \mathbf{c} &= \left(\mathbf{I} - \mathbf{G}\hat{\mathbf{H}}\right) E\{\mathbf{a}\}. \end{aligned}$$

Here $\mathbf{I}$ denotes the $N_R \times N_R$ identity matrix. A derivation for the receiver following our system model with non-zero mean data (on-off keying) is found in the Appendix A.

3) Ordered Successive Cancellation (OSUC) Receiver: Another approach follows the above described idea of a cancellation receiver [20]. First the strongest signal component, characterised by $\max_i ||\hat{\mathbf{H}}(:,i)||_F$, is decoded, using either an MMSE or ZF receiver as proposed above (in the simulations in Section VI it uses the MMSE). Here, $\|\cdot\|_F$ denotes the Frobenius norm, and $\hat{\mathbf{H}}(:,i)$ denotes the i'th column of $\hat{\mathbf{H}}$. Thereafter, the signal is remodulated and subtracted from the constellation. Assuming, this decoding was correct, the remaining constellation only consists of components of the second tag signal.

4) Separate and Combine (S&C) Receiver: Another receiver proposed for comparison is what we call *Separate and Combine*. This receiver separates the signal components on each receive antenna individually, utilising the proposed single antenna zero-forcing receiver. Thereafter, the signals from each antenna, belonging to the same tag i are combined using maximal ratio combining:

$$\hat{s}_i = \frac{1}{|\tilde{h}_{i1}|^2 + |\tilde{h}_{i2}|^2} \left(\tilde{h}_{i1}^* \tilde{s}_{i1} + \tilde{h}_{i2}^* \tilde{s}_{i2} \right), \tag{20}$$

where $\tilde{h}_{1j} = \tilde{S}_{1j}^{(r)} - \tilde{S}_{1j}^{(a)}$ and $\tilde{h}_{2j} = \tilde{S}_{2j}^{(r)} - \tilde{S}_{2j}^{(a)}$ are the channel coefficients h_{1j} and h_{2j} for each antenna j, projected into the subspaces $S_{2\perp}$ and $S_{1\perp}$, respectively (Fig. 6). The asterisk * denotes the conjugate complex of the value. It is shown in Section VI that for a $N_R \times R = 2 \times 2$ system the average performance of the S&C and ZF receivers is equal.

We observe, that in case of a collision, the reception of both tag sequences does not increase the throughput, compared to the reception of just one of the signals, since a conventional transmitter can only acknowledge one tag at a time

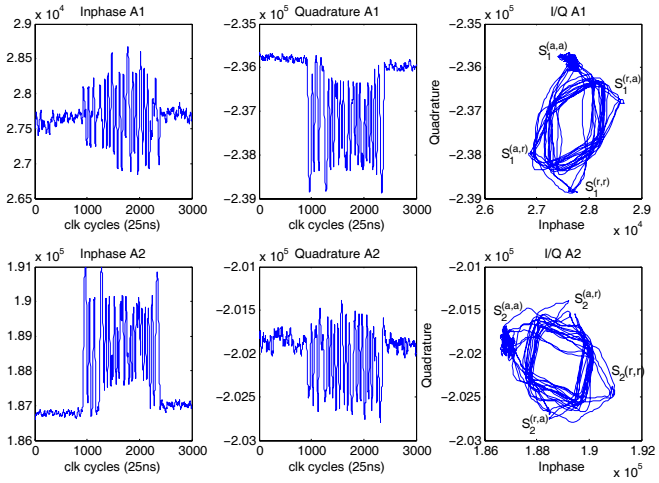

Fig. 8. Baseband signals of measurement data of collision with two tags.

($M = 2$, $J = 1$). In this situation the reader only decodes the stronger of the two tag signals, given by $\max_i |h_i|$ and $\max_i ||\mathbf{H}(:,i)||_F$ for the single and dual antenna receivers, respectively. Clearly, successive cancellation receivers do not provide any performance benefit in that case. However, if the reader manages to acknowledge both tags (either by changing the standard to acknowledge several tags consecutively, or by exploiting spatial separation of the tags using transmit precoding), we can exploit the reception of both tags to increase the throughput as given in Equation (4).

The proposed channel estimation and single antenna receivers are restricted to a separation of two tag signals ($M = 2$). Assuming the channel matrix is known for a collision with more than two tags, the multiple antenna ZF, MMSE and OSUC receivers are capable to recover also from collisions with $R > 2$, as long as $R \leq N_R$. In that case, the channel matrix $\mathbf{H}$ in the corresponding Equations (18) and (19) is of dimension $N_R \times R$.

V. Verification with Measurement Data

In order to verify both, our collision model for two tags in one slot, as well as the proposed receivers, we run our algorithms on measurement data of collisions with two commercially available tags [21]. The measurement data was recorded on our RFID prototyping environment [22]–[24], which is composed of a digital baseband processing part and analogue radio-frequency frontends. The measurement was conducted indoor in an environment with a strong Line Of Sight (LOS) component and almost no fading, with reader to tag distances of 2.3 m and 1.7 m. The transmitter and both receivers were decoupled by using separate antennas, with gains of 9 dBi and 8 dBi, respectively. Further details of the setup for recording the measurement data and the underlying hardware are given in Section IV of [24]. The tags are activated by a `QUERY` command from the reader, and the collided 16 bit random number packets (`RN16`) of the tags at two reader receive antennas are captured after Analogue-to-Digital-Converters (ADC) and imported into Matlab for offline processing. Figure 8 shows the measurement data of the inphase and quadrature component in the time domain, as

well as the I/Q constellation of the collision, for both antennas. Clearly, we can again determine the various states $S_j^{(a,a)}$, $S_j^{(a,r)}$, $S_j^{(r,a)}$ and $S_j^{(r,r)}$. As assumed in our model, the data samples are located within the area defined by those states. As the modulation signal of both tags is not synchronous, the receive signal moves on trajectories, that are not directly connecting the states, as mentioned in Section III (mainly due to the delay τ_i in the example of Fig. 8).

We applied our proposed channel estimation algorithm, which correctly detects the appropriate states in the constellation of the measurement data. Furthermore, we applied all receivers of both classes, the single antenna receivers as well as the multiple antenna receivers. Figure 7 shows the resolved sequences of the example using the single antenna zero-forcing receiver: The two subplots show the two projected signals $\tilde{s}_i$ into the orthogonal subspace of the interfering signal. The interference is completely canceled. Each of these resolved signals are thereafter synchronised and decoded individually.

Although the tag sequences can be decoded, a major drawback of the result is, that it is not possible to prove that the resolved sequences are decoded correctly, as the data transmitted by the tags is random (tags transmit a 16 bit random number). A justification for a correct functionality however is, that the separated signals are obviously two independent, correctly encoded FM0 sequences with a valid preamble, as the reader expects them. To further validate our algorithms, the following section provides simulation results, and clearly we can verify the correct decoding of the data and the functionality of the algorithms in simulation. The assumptions in the simulation and the previously proposed model are corroborated by the measurement data. Although all receivers show a cancellation of the interfering tag sequences, we exemplarily only plot the separated sequences of the SAZF receiver in Fig. 7. The following performance simulations show, that this receiver actually exhibits the worst performance among all the proposed receivers.

VI. Performance Analysis

In order to compare the performance of the various proposed receivers, we compute the Bit Error Ratio (BER) using Monte Carlo simulations of slots with two tag responses. Two receive antennas are assumed in our simulations for all multiple antenna receivers.

A. Rayleigh-Fading Channel

For the sake of a simple comparison and analytic tractability, we assume that the equivalent channel matrix $\mathbf{H}$ follows a Rayleigh fading. The single Rayleigh channel coefficients are independent zero mean circularly symmetric complex Gaussian random variables with normalised energy $E\{|h_i|^2\} = 1$, which implies that the two tags participating in the collision experience the same path loss. Figure 9 shows the performance of the various Single Antenna (SA) and dual antenna receivers, decoding both tag signals of uncoded random data depending on the average output SNR $\bar{\gamma} = 1/N_R \sum_j \bar{\gamma}_j$, where $\gamma_j = |h_{i,j}|^2 a_i^2/N_0$ is the instantaneous SNR at antenna j for tag i, and $\bar{\gamma}_j = E\{\gamma_j\}$ is the average SNR at antenna j.

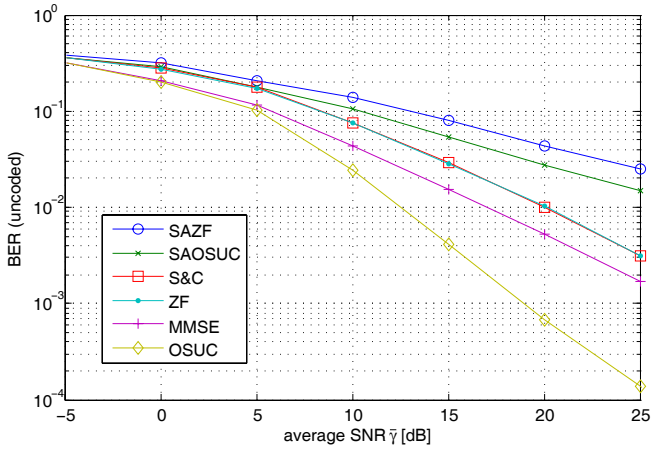

Fig. 9. Bit Error Ratio for single and multiple antenna receivers in Rayleigh fading channel in collision slots of two tags (R=2). In the simulation, *both* tag sequences are resolved.

Additionally to disturbance by noise, each stream is interfered by the second tag responding in the same slot, with the same average signal power, and the carrier leakage. The interference from other tags as well the carrier leakage however, have a different impact on the performance than the noise, as they are assumed to be known (estimated) to the receiver.

As expected, the multiple antenna receivers outperform the single antenna receivers. Furthermore, the simple ZF receivers show a worse performance than the MMSE and OSUC (using MMSE for decoding the first stream) receivers.

Furthermore, we analyse the performance of the SAZF receiver analytically: as stated in Section IV-B1 and depicted in Fig. 6, the effective receive signal $\tilde{s}_i$ is degraded by the projection loss. In a first step we calculate the statistics of this projected receive signal

$$\tilde{s}_i = s_i \sin(\varphi_1 - \varphi_2), \tag{21}$$

where s_i follows a Rayleigh distribution and $\varphi_1 - \varphi_2$ is equally distributed in $(-\pi, \pi]$. Using the statistical independence of the two random variables, the probability density function of the projected signal $\tilde{s}_i$ is calculated by transforming the random variables [25, p. 446]. Hence, in case of Rayleigh fading on the channel, the statistics of $\tilde{s}_i$ are transformed into a Gaussian fading. Equally, the projected channel coefficients $\tilde{h}_{ij}$ follow a Gaussian fading, with $E\{|\tilde{h}_{ij}|^2\} = 1/2\, E\{|h_{ij}|^2\}$.

The Bit Error Probability (BEP) for each tag signal is calculated as

$$P_b(E) = \int_0^\infty P_b(E|\gamma) p_\gamma(\gamma) d\gamma, \tag{22}$$

where we skip the index of the instantaneous SNR γ as there is only a single antenna. As the modulation follows an on-off keying, the conditional BEP $P_b(E|\gamma)$ is:

$$P_b(E|\gamma) = Q(\sqrt{\gamma}), \tag{23}$$

where $Q(\cdot)$ denotes the Q-function. Using the alternative description of the Q-Function from [26] and following the approach of Alouini *et al.* [27], the diversity order in collision slots with two tags for the single antenna ZF receiver is

derived to be $1/2$, while the diversity order of the dual antenna ZF receiver is well known to be $N_R - R + 1 = 1$ [10]. Thus, by doubling the number of receive antennas from the SAZF receiver to the dual antenna ZF receiver, also the diversity order is doubled. The evaluation of the integral in Equation (22) is shown in Appendix B.

With the Separate-and-Combine (S&C) receiver, we can again improve the diversity order to one. In fact the average performance of the S&C receiver and the ZF receiver is equal: In order to show that, we compare the post-processing SNR at the output of the two receivers. As both receivers scale the signal power at the output equally, the post processing SNR is equal to the post processing noise power.

We first compute the noise power $\sigma^2_{ZF,i}$ of the i'th output stream of the ZF receiver, which is the element in the i'th row and i'th column (denoted by the subscript $_{ii}$) of the matrix:

$$\begin{aligned} E\left\{\mathbf{n}_{ZF}\mathbf{n}_{ZF}^H\right\} &= E\left\{(\mathbf{H}^H\mathbf{H})^{-1}\mathbf{H}^H\mathbf{n}\mathbf{n}^H\mathbf{H}((\mathbf{H}^H\mathbf{H})^{-1})^H\right\} \\ &= \sigma_n^2 E\left\{((\mathbf{H}^H\mathbf{H})^{-1})^H\right\}, \\ \sigma^2_{ZF,i} &= \sigma_n^2 E\left\{(\mathbf{H}^H\mathbf{H})^{-1}\right\}_{ii}. \end{aligned} \tag{24}$$

It has been shown by Winters *et al.* [28] and Gore *et al.* [29], that the term $1/\{(\mathbf{H}^H\mathbf{H})^{-1}\}_{ii}$ follows a Chi-Square distribution with $N_R - R + 1$ degrees of freedom. Thus, in our case of $N_R = R = 2$ the expected value in Equation (24) is:

$$E\left\{(\mathbf{H}^H\mathbf{H})^{-1}\right\}_{ii} = \frac{1}{\sigma_h^2}, \tag{25}$$

with $\sigma_h^2 = E\{|h_{ij}|^2\}$. Hence, the post processing noise power is $\sigma^2_{ZF,i} = \sigma_n^2/\sigma_h^2$.

Reviewing Equation (20), the noise $n_{S\&C,i}$ at the i'th output stream of the S&C receiver calculates to:

$$n_{S\&C,i} = \frac{1}{\tilde{\mathbf{h}}_i^H\tilde{\mathbf{h}}_i}\left(\tilde{\mathbf{h}}_i^H\mathbf{n}\right). \tag{26}$$

Here, we stack the elements $\tilde{h_{ij}}$ of Equation (20) into the $N_R \times 1$ vector $\tilde{\mathbf{h}}_i$. The noise power $\sigma^2_{S\&C,i}$ at the i'th output stream of the S&C receiver hence is:

$$\sigma^2_{S\&C,i} = E\left\{\frac{|\tilde{\mathbf{h}}_i^H\mathbf{n}|^2}{|\tilde{\mathbf{h}}_i^H\tilde{\mathbf{h}}_i|^2}\right\} = \sigma_n^2\, E\left\{\frac{1}{\tilde{\mathbf{h}}_i^H\tilde{\mathbf{h}}_i}\right\}. \tag{27}$$

As the single elements $\tilde{h}_{ij}$ exhibit independent Gaussian fading, and $E\{|\tilde{h}_{ij}|^2\} = 1/2\, E\{|h_{ij}|^2\}$ it follows that $\tilde{\mathbf{h}}_i^H\tilde{\mathbf{h}}_i$ is Chi-square distributed with N_R degrees of freedom and $E\{\tilde{\mathbf{h}}_i^H\tilde{\mathbf{h}}_i\} = N_R\sigma_h^2/2$. Thus, in our case of $N_R = 2$, the noise power of the i'th stream at the output of the S&C receiver is $\sigma^2_{S\&C,i} = \sigma_n^2/\sigma_h^2$. Hence, the average post-processing SNR of both receivers is equivalent, resulting in the same average performance in the case of $N_R \times R = 2 \times 2$. However, if we increased the number of receive antennas, we could exploit a higher diversity order with the zero-forcing receiver.

B. Dyadic Backscatter Channel

Finally, we simulate the performance of the various receivers in the dyadic backscatter channel [30], assuming the fading of the forward ($\mathbf{h}^f$) and backward ($\mathbf{H}^b$) links to be uncorrelated, and perfect on-off keying modulation at the tags, i.e. $\sqrt{\Delta\sigma_i} = 1$. Channel measurements carried out by Lázaro et al. [31] and Kim *et al.* [32] propose the use of a two-way Rician channel model, which is intuitive in RFID scenarios. They however point out, that the Rician factor strongly depends on the environment, and in some scenarios, the best fit to the measurement data was achieved by applying a two-way Rayleigh distribution. As the Rayleigh fading model also serves as a lower bound for the Rician fading model, we stick to this assumption in our simulations. Both, forward and backward links, as well as both tags of the collision, are assumed to experience the same path loss. The data packets are FM0 encoded 16 bit random numbers as defined in [2].

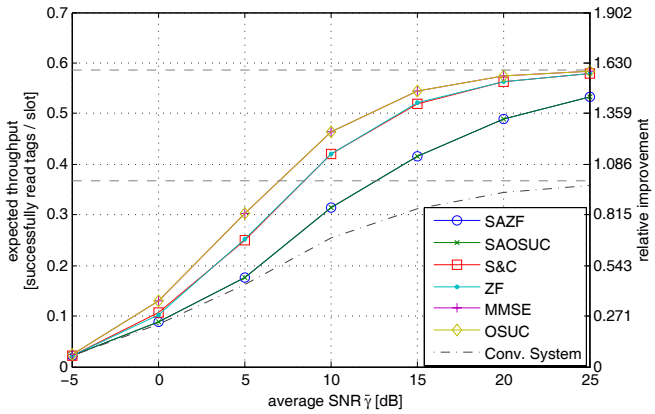

Fig. 10. Expected throughput of the FSA scheme with the capability to recover from a slot with two tags and acknowledge one tag (M=2, J=1) for the various proposed receivers. Moreover, the graph shows the relative improvement over the theoretical throughput of the conventional system (0.368 tags/slot). The two dashed horizontal lines indicate the theoretical throughput of M=1, J=1 and M=2, J=1. The grey curve plots the throughput of the conventional system with a single receive antenna with ML-sequence decoding for comparison.

Figure 10 shows the expected throughput of the receivers and the relative improvement to the theoretical throughput of the conventional system (0.368 tags / slot) in the FSA framework for $M = 2$, $J = 1$, as described in Section II. The receivers only decode one of the two packets involved in the collision, i.e. the one with the stronger receive signal, as discussed in Section IV. In case of a slot with a single tag response, we assume Maximum Likelihood (ML) sequence decoding of the FM0 code for the single antenna receivers [33], and Maximal Ratio Combining (MRC) for the dual antenna case. We observe that the successive cancellation receivers do not show any further performance increase to the ZF or MMSE receivers, if we are only interested in decoding one of the packets of the collision slot. The multiple antenna receivers show a better performance than the single antenna receivers. For high $\bar{\gamma}$ the expected throughput converges towards 0.587, or equivalently, to a relative improvement of 1.595 times the theoretical throughput of the conventional system. For comparison, we also plot the throughput of the conventional system (M=1, J=1) assuming ML sequence decoding [33].

Links with a correlation between the forward and the backward channel have been studied by Griffin *et al.* in [11]. They conclude, that the performance loss is small if the link

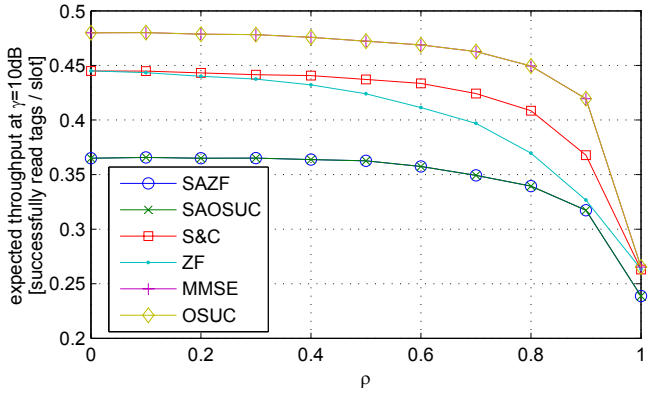

Fig. 11. Expected throughput of FSA scheme (M=2, J=1) for the various proposed receivers with tag antenna correlation, at $\bar{\gamma} = 10\,\text{dB}$.

envelope correlation $\rho_e < 0.6$, which is assumed for setups with sufficiently separated transmit and receive antennas, thus this is not considered here. Moreover, antenna correlation may be caused by not sufficient scattering and closely spaced antennas. In RFID scenarios we expect that the reader receive antenna correlation is small due to sufficient spacing, while the tag correlation impacts most due to potentially close tag locations. This is modeled by [10, Chapter 3]: $\mathbf{H}^b = \mathbf{H}^b_{uc}\mathbf{R}_t^{1/2}$ and $\mathbf{h}^f = \mathbf{R}_t^{1/2}\mathbf{h}^f_{uc}$, where $\mathbf{R}_t$ is the tag covariance matrix, and $\mathbf{H}^b_{uc}$ and $\mathbf{h}^f_{uc}$ are the backward and forward channel matrix with independent Rayleigh fading, respectively. Figure 11 shows the expected loss in case of tag antenna correlation at $\bar{\gamma} = 10\,\text{dB}$, with $\{\mathbf{R}_r\}_{ii} = 1$ and $\{\mathbf{R}_r\}_{ij} = \rho$ for $i \neq j$. At $\rho = 0$ the throughput is the same as at 10 dB SNR of Fig. 10, while with full correlation $\rho = 1$ only the throughput of the single slots is achieved (MRC and ML sequence decoding in case of multiple and single antenna receivers, respectively). As the S&C receiver separates the signals in the I/Q plane, it is less affected by the antenna correlation as the ZF receiver, which utilises the spatial signatures of the signals. We observe that for $\rho < 0.6$ the system losses in terms of throughput are marginal.

The authors however want to explicitily point out, that they are not aware of any experimental work that investigates the amount of correlation in the dyadic pinhole channel in realistic scenarios, thus the result should provide an impression on the expected losses in case of existing antenna correlations. The extent of the correlation however is expected to depend strongly on the setup and environment, and experimental research on this topic is suggested for future work.

VII. Discussion and Conclusion

In this work we identify the theoretical throughput increase of FSA RFID systems with physical layer collision recovery receivers. For a receiver capable of successfully reading and acknowledging one tag of a slot with two tags, a throughput increase of approximately 1.6 times the throughput of a conventional RFID reader is achieved. The authors note, that FSA with physical layer collision recovery is feasible in RFID, as all receive signal components are modulated to the very same carrier frequency. With that potential being identified, we develop an accurate model for tag collisions and baseband constellations in RFID readers, which enables us to propose a channel estimation and leads us to the development of the desired receivers. We identify two main challenges for UHF RFID systems: First, the tags participating in the collision feature highly distinct symbol rates, due to large tolerances for RFID tags. And second, the tag signals are disturbed by a strong carrier leakage. The channel estimation for $M = 2$ as well as the receivers proposed, are capable of handling these specifics of RFID systems, and assume a slowly changing carrier leakage and channel (block fading), which is true in many realistic RFID scenarios. The validity of the assumptions is corroborated by measurement data.

The two presented classes of receivers either discriminate the tag signals in the I/Q constellation (single antenna case) or exploit their different spatial signatures (multiple antenna case). The performance of the proposed receivers is analysed analytically and by means of Monte Carlo simulations. As expected, multiple antenna receivers feature higher performance at the tradeoff of higher signal processing complexity. The SAZF receiver shows a diversity order of $1/2$. Combining the signals of two SAZF receiver outputs (S&C) allows to reconstitute the diversity order of 1, which is known to be equal to the diversity order of the dual antenna ZF receiver. We observe that the proposed channel estimation and single antenna receivers are only capable of recovering from collisions of two tags, while the multiple antenna receivers may recover from a collision of up to M tags if $N_R \geq M$ receive antennas are available and the channel is known at the receiver.

The increased data throughput of the system comes with a complexity increase at the RFID reader only. Furthermore, the receivers do not require any changes in existing RFID standards, and hence can be directly implemented in RFID receivers to work with commercially available tags, as shown by our measurement data. Although this work concentrates on FSA, the receivers can be equally applied to the binary tree anti collision protocol. Equivalently, this work can be applied to other systems communicating with backscatter technology, such as wireless sensor networks.

For future work in this new research field it is intended to investigate channel estimation for multiple tag collisions involving even more than two tags ($M > 2$), which then allows to employ multiple antenna receivers to split more than two tags. Additionally, the applicability of multiple antenna transmitters for precoding and thereby acknowledging multiple tags simultaneously ($J > 1$) needs thorough investigation. This also requires models and experimental investigation of correlations between multiple antenna forward and backward channels in different setups. Finally, together with [4], [5], this work opens potential for higher performance tag population estimators, which utilise the physical layer information of the *exact* number of tags responding in a slot with $R \leq M$.

Appendix A
Derivation of MMSE Receiver

Following [34], the MMSE receiver of the form

$$\hat{\mathbf{s}}_{MMSE} = \mathbf{G}(\mathbf{s} - \hat{\mathbf{l}}) + \mathbf{c} \tag{28}$$

is based on two conditions: first, the orthogonality principle:

$$E\{(\mathbf{a} - \hat{\mathbf{s}}_{MMSE})(\mathbf{s} - \hat{\mathbf{l}})^H\} = 0, \tag{29}$$

and second, the condition for an unbiased receiver:

$$E\{\mathbf{a} - \hat{\mathbf{s}}_{MMSE}\} = 0. \tag{30}$$

Inserting Equation (12) in Equation (30) leads to the result

$$\mathbf{c} = \left(\mathbf{I} - \mathbf{G}\hat{\mathbf{H}}\right) E\{\mathbf{a}\}. \tag{31}$$

Proceeding with the insertion of Equations (28) and (12) into the first condition (Equation (29)), results in:

$$\mathbf{G} = \mathbf{C}_{aa}\hat{\mathbf{H}}^H(\hat{\mathbf{H}}\mathbf{C}_{aa}\hat{\mathbf{H}}^H + N_0\mathbf{I})^{-1}, \tag{32}$$

where $\mathbf{C}_{aa} = E\{(\mathbf{a} - E\{\mathbf{a}\})(\mathbf{a} - E\{\mathbf{a}\})^H\}$ denotes the covariance matrix of the data. Due to the on-off keying modulation, we find $\mathbf{C}_{aa} = \frac{1}{4}\mathbf{I}$. Equation (32) is finally reformulated to:

$$\mathbf{G} = \hat{\mathbf{H}}^H(\hat{\mathbf{H}}\hat{\mathbf{H}}^H + 4N_0\mathbf{I})^{-1}. \tag{33}$$

APPENDIX B
DERIVATION OF DIVERSITY ORDER FOR SINGLE ANTENNA ZERO FORCING RECEIVER

We start by using the alternative description of the Q-function by Craig [26]

$$Q(x) = \frac{1}{\pi}\int_0^{\pi/2} \exp\left(-\frac{x^2}{2\sin^2\phi}\right) d\phi, \tag{34}$$

and the approach shown by Alouini *et al*. [27]. With the Gaussian distribution for the fading of the projected signal $\tilde{s}_i$, the distribution $p_\gamma(\gamma)$ of the instantaneous SNR γ follows a Gamma distribution. Inserting the description of the Q-function in Equation (34) into Equation (22), the bit error probability is:

$$P_b(E) = \frac{1}{\pi}\int_0^{\infty}\int_0^{\pi/2} \exp\left(\frac{-\gamma}{2\sin^2\phi}\right) d\phi\, p_\gamma(\gamma) d\gamma. \tag{35}$$

Changing the order of integration, the inner integral gives the moment generating function of the Gamma distribution, which is found in [27, Eq. (30)]. Hence, the BEP yields:

$$\begin{aligned} P_b(E) &= \frac{1}{\pi}\int_0^{\pi/2}\left(1 + \frac{\bar{\gamma}}{\sin^2\phi}\right)^{-1/2} d\phi. \qquad (36)\\ &= \frac{1}{\pi\sqrt{\bar{\gamma}}}\int_0^{\pi/2}\left(\frac{\sin^2\phi}{\frac{\sin^2\phi}{\bar{\gamma}} + 1}\right)^{1/2} d\phi. \end{aligned}$$

With $\lim_{(\bar{\gamma}\to\infty)} \frac{\sin^2\phi}{\bar{\gamma}} = 0$, the BEP for large $\bar{\gamma}$ becomes

$$P_b(E) \cong \frac{1}{\pi}\bar{\gamma}^{-1/2}. \tag{37}$$

Hence, at high SNR $\overline{\gamma}$, the diversity order of the single antenna zero-forcing receiver is found to be $1/2$.

ACKNOWLEDGMENT

This work has been funded by the Christian Doppler Laboratory for Wireless Technologies for Sustainable Mobility, the Federal Ministry of Economy, Family and Youth and the National Foundation for Research, Technology and Development of Austria. The authors thank Christoph Mecklenbräuker and Georg Maier for their valuable support, and our industrial partner Infineon for enabling that work. The authors are grateful for the numerous suggestions and comments by the anonymous reviewers.

REFERENCES

[1] C. Angerer, G. Maier, M. V. Bueno-Delgado, M. Rupp, and J. Vales-Alonso, "Single antenna physical layer collision recovery receivers for RFID readers," in *Proc. IEEE International Conf. Industrial Technology*, Mar. 2010, pp. 1386–1391.

[2] EPCglobal, "EPC radio-frequency identity protocols Class-1 Generation-2 UHF RFID." [Online]. Available: http://www.epcglobalinc.org

[3] M. V. Bueno-Delgado, J. Vales-Alonso, and F. J. Gonzalez-Castano, "Analysis of DFSA anti-collision protocols in passive RFID environments," in *Proc. 35th Conf. IEEE Industial Electronics Society (IECON)*, Nov. 2009.

[4] R. S. Khasgiwale, R. U. Adyanthaya, and D. W. Engels, "Extracting information from tag collisions," in *Proc. IEEE International Conf. RFID*, Apr. 2009.

[5] D. Shen, G. Woo, D. P. Reed, A. B. Lippman, and J. Wang, "Separation of multiple passive RFID signals using software defined radio," in *Proc. IEEE International Conf. RFID*, Apr. 2009.

[6] J. Yu, K. H. Liu, X. Huang, and G. Yan, "An anti-collision algorithm based on smart antenna in RFID system," in *Proc. International Conf. Microwave Millimeter Wave Technol. ICMMT*, Apr. 2008, vol. 3, pp. 1149–1152.

[7] J. Lee, T. Kwon, Y. Choi, S. K. Das, and K. Kim, "Analysis of RFID anti-collision algorithms using smart antennas," in *Proc. International Conf. Embedded Networked Sensor Syst.*, 2004.

[8] A. F. Mindikoglu and A.-J. van der Veen, "Separation of overlapping RFID signals by antenna arrays," in *Proc. IEEE International Conf. Acoustics, Speech Signal Processing, ICASSP*, Apr. 2008, pp. 2737–2740.

[9] N. Abramson, "Packet switching with satellites," in *Proc. National Computer Conf. Exposition*, June 1973.

[10] A. Paulraj, R. Nabar, and D. Gore, *Introduction to Space-Time Wireless Communication*. Cambridge University Press, 2003.

[11] J. D. Griffin and G. D. Durgin, "Link envelope correlation in the backscatter channel," *IEEE Commun. Lett.*, vol. 11, no. 9, pp. 735–737, 2007.

[12] D.-Y. Kim, H.-S. Jo, H. Yoon, C. Mun, B.-J. Jang, and J.-G. Yook, "Reverse-link interrogation range of a UHF MIMO-RFID system in Nakagami-m fading channels," *IEEE Trans. Ind. Electron.*, vol. 57, no. 4, pp. 1468–1477, Apr. 2010.

[13] P. V. Nikitin, K. V. S. Rao, and R. D. Martinez, "Differential RCS of RFID tag," *Electron. Lett.*, vol. 43, no. 8, Apr. 2007.

[14] Impinj, "Gen 2 tag clock rate–what you need to know," 2005.

[15] D. M. Dobkin, *The RF in RFID: Passive UHF RFID in Practice*. Elsevier, 2008.

[16] G. Lasser, R. Langwieser, and A. L. Scholtz, "Broadband suppression properties of active leaking carrier cancellers," in *Proc. IEEE International Conf. RFID*, Apr. 2009.

[17] B. Knerr, M. Holzer, C. Angerer, and M. Rupp, "Slot-wise maximum likelihood estimation of the tag population size in FSA protocols," *IEEE Trans. Commun.*, vol. 58, pp. 578–585, Feb. 2010.

[18] C. Angerer, R. Langwieser, G. Maier, and M. Rupp, "Maximal ratio combining receivers for dual antenna RFID readers," in *Proc. IEEE MTT-S International Microwave Workshop Wireless Sensing, Local Positioning, RFID*, Sep. 2009, pp. 21–24.

[19] P. Patel and J. Holtzman, "Analysis of a simple successive interference cancellation scheme in a DS/CDMA system," *IEEE J. Sel. Areas Commun.*, vol. 12, no. 5, pp. 796–807, June 1994.

[20] G. Golden, G. Foschini, R. Valenzuela, and P. Wolniansky, "Detection algorithm and initial laboratory results using V-BLAST space time communication architecture," *Electron. Lett.*, vol. 35, no. 1, pp. 14–16, Jan. 1999.

[21] UPM Raflatac, RFID, "Rafsec web paper tag, global UHF C1G2 EPC," May 2007, Product Specification, Version 1.1.

[22] C. Angerer, B. Knerr, M. Holzer, A. Adalan, and M. Rupp, "Flexible simulation and prototyping for RFID designs," in *Proc. 1st International EURASIP Workshop RFID Technology, RFID*, Sep. 2007, pp. 51–54.

[23] C. Angerer, M. Holzer, B. Knerr, and M. Rupp, "A flexible dual frequency testbed for RFID," in *Proc. 4th International Conf. Testbeds Research Infrastructures Development Networks Communities*, 2008.

[24] R. Langwieser, C. Angerer, and A. L. Scholtz, "A UHF frontend for MIMO applications in RFID," in *Proc. IEEE Radio and Wireless Symposium*, Jan. 2010, pp. 124–127.

[25] T. K. Moon and W. C. Stirling, *Mathemetical Methods and Algorithms for Signal Processing*. Prentice Hall, 2000.

[26] J. W. Craig, "A new, simple and exact result for calculating the probability of error for two-dimensional signal constellations," in *Proc. IEEE Military Commun. Conf.*, 1991, pp. 571–575.
[27] M. S. Alouini and A. J. Goldsmith, "A unified approach for calculating error rates of linearly modulated signals over generalized fading channels," *IEEE Trans. Commun.*, vol. 47, no. 8, Sep. 1999.
[28] J. H. Winters, J. Salz, and R. D. Gitlin, "The impact of antenna diversity on the capacity of wireless communication systems," *IEEE Trans. Commun.*, vol. 42, no. 2/3/4, Feb./Mar./Apr. 1994.
[29] D. Gore, R. W. Heath, and A. Paulraj, "On performance of the zero forcing receiver in presence of transmit correlation," in *Proc. IEEE International Symposium Information Theory.*, 2002.
[30] J. D. Griffin and G. D. Durgin, "Gains for RF tags using multiple antennas," *IEEE Trans. Antennas Propagat.*, vol. 56, no. 2, pp. 563–570, Feb. 2008.
[31] A. Lázaro, D. Girbau, and D. Salinas, "Radio link budgets for UHF RFID on multipath environments," *IEEE Trans. Antennas Propagat.*, vol. 57, no. 4, pp. 1241–1251, Apr. 2009.
[32] D. Kim, M. A. Ingram, and W. W. Smith, "Measurements of small-scale fading and path loss for long range RF tags," *IEEE Trans. Antennas Propagat.*, vol. 51, no. 8, Aug. 2003.
[33] M. Simon and D. Divsalar, "Some interesting observations for certain line codes with application to RFID," *IEEE Trans. Commun.*, vol. 54, no. 4, Apr. 2006.
[34] S. M. Kay, *Fundamentals of Statistical Signal Processing: Estimation Theory*. Prentice Hall, 1993.

Christoph Angerer received his Dipl.-Ing. degree in electrical engineering from the Vienna University of Technology in 2005, with distinction. For his master degree he collaborated with the Forschungszentrum Telekommunikation Wien (FTW). After he spent one and a half years in industry with embedded system design, he started working towards his PhD. He is a member of the Christian Doppler Laboratory for Wireless Technologies for Sustainable Mobility at the Institute for Communications and Radio Frequency Engineering at the Vienna University of Technology. His research interests include radio frequency identification, embedded systems, wireless communications, digital signal processing, and its implementation.

Robert Langwieser studied electrical engineering with emphasis on radio-frequency engineering at the Vienna University of Technology in Austria. He received there his master degree in 2004 and his Doctor degree in 2009, both with distinction. Since 2004, Mr. Langwieser has been employed as a research assistant at the Institute of Communications and Radio-Frequency Engineering at the same university. From 2004 to 2009, he was a staff member of the Christian Doppler Laboratory for Design Methodology of Signal Processing Algorithms, and since July 2009, he has been a staff member of the newly founded Christian Doppler Laboratory for Wireless Technologies for Sustainable Mobility. His research is focused on the development of modular and flexible radio frontends for rapid prototyping and measurement systems especially for multiple input multiple output (MIMO) scenarios.

Markus Rupp received his Dipl.-Ing. degree in 1988 at the University of Saarbruecken, Germany, and his Dr.-Ing. degree in 1993 at the Technische Universitaet Darmstadt, Germany, where he worked with Eberhardt Haensler on designing new algorithms for acoustical and electrical echo compensation. From November 1993 until July 1995, he had a postdoctoral position at the University of Santa Barbara, California, with Sanjit Mitra, where he worked with Ali H. Sayed on a robustness description of adaptive filters with impact on neural networks and active noise control. From October 1995 until August 2001, he was a Member of Technical Staff in the Wireless Technology Research Department of Bell-Labs at Crawford Hill, NJ, where he worked on various topics related to adaptive equalization and rapid implementation for IS-136, 802.11, and UMTS. Since October 2001, he has been a full professor for Digital Signal Processing in Mobile Communications at the Vienna University of Technology, where he founded the Christian-Doppler Laboratory for Design Methodology of Signal Processing Algorithms in 2002 at the Institute for Communications and RF Engineering. He served as Dean from 2005-2007. He was an associate editor of the IEEE TRANSACTIONS ON SIGNAL PROCESSING from 2002-2005, and is currently an associate editor of the *JASP EURASIP Journal of Advances in Signal Processing* and the *JES EURASIP Journal on Embedded Systems*. He is an elected AdCom member of EURASIP since 2004, serving as president of EURASIP from 2009-2010. He has authored and co-authored more than 300 papers and patents on adaptive filtering, wireless communications, and rapid prototyping, as well as automatic design methods.